MINIATURIZED IMPRESSION CREEP TESTING OF BALL GRID ARRAY (BGA) SOLDER BALLS ATTACHED TO MICRO-ELECTRONIC PACKAGING SUBSTRATES

Deng Pan, Robert A. Marks, and Indranath Dutta

Center for Materials Science and Engineering, Department of Mechanical Engineering, Naval Postgraduate School, Monterey, CA 93943

Susheel G. Jadhav

Intel Corporation, 5000 West Chandler Boulevard, MS CH5-165, Chandler, AZ 85226

Abstract

This paper reports on the design and implementation of a miniaturized impression creep apparatus for characterizing the creep behavior of tiny solder balls attached to a ball grid array (BGA) microelectronic packaging substrate. The technique requires no special sample preparation, can probe individual solder balls, and proffers high data throughput by allowing numerous creep curves to be obtained from one substrate, as well as by minimizing the time required to achieve steady state creep. The apparatus reported here uses a 100μm diameter cylindrical WC punch to characterize the creep behavior of 750μm diameter BGA solder balls from ambient temperature to 423K. A video imaging system facilitates precise alignment and placement of the indenter on the specimen at the test temperature. The possible effect of substrate curvature on the experimental solder creep curves was evaluated and was deemed to be insignificant. Example creep curves and data based on 90Pb-10Sn BGA solder balls are presented. The test is further scaleable for testing of smaller flip-chip (FC) joints, using a smaller punch. The present work constitutes the first known report on the successful implementation of impression creep for testing non-bulk specimens.

I. Introduction

Microelectronic solder joints in service are exposed to severe thermo-mechanical cycling (TMC) and suffer low-cycle fatigue failure due to the thermal expansion mismatch between different parts of a microelectronic package (e.g., the Si chip and the organic circuit board or substrate). As a consequence, the creep properties of the solder material play a key role in the performance and durability of flip chip (FC) and ball grid array (BGA) solder joints. With continuing emergence of new generations of lead-free solders (e.g. Sn-Ag or Sn-Ag-Cu) to replace conventional lead-bearing solders for environmental reasons, significant current interest has been focused on developing approaches for efficiently characterizing the creep behavior of various candidate Pb-free solder materials [1-5].

The creep characterization of microelectronic solders is complicated by several factors. First, the microstructures of materials such as Sn-Ag and Sn-Ag-Cu have been found to be strongly dependent on cooling rate [6], and hence, specimen size [7] during processing. Secondly, since microelectronic solder balls are attached to chips or substrates through bond-pads of either Cu or Ni, which have significant solubilities in liquid Sn, the actual composition of FC or BGA balls, and consequently their mechanical properties, are often quite different from that of pure solder [12]. Hence, in order to enable accurate reliability prediction of microelectronic solder joints, it is crucial to characterize the creep behavior of either small material volumes simulating individual solder balls, or preferably, of the solder joints themselves following attachment to the packaging substrate or the chip.

Additionally, the creep behavior of solder joints in microelectronic packages may change continuously as a result of both static isothermal aging-induced phase coarsening, as well as strain-enhanced coarsening of second phase particles [8-11]. This necessitates that creep tests be completed in relatively short times, so that there is no significant microstructural (and hence property) change during a given test.

In order to address the need to test actual solder joints, the lap-shear specimen, which allows simultaneous testing of an array of solder balls (typically numbering ~ 50-100) in nominal shear, has been widely utilized [13,14]. Although the lap-shear approach alleviates the difficulties in

studying bulk solders, it has several limitations. First, the sample geometry requires the preparation of specially designed specimens, which can be complicated and expensive. Secondly, each sample yields only a few creep curves at best, requiring numerous samples for complete material characterization. Thirdly, like conventional creep tests, these tests take long times to complete, potentially allowing *in situ* microstructural changes to occur during a test. Fourthly, and probably most importantly, creep tests based on lap-shear frequently display a prolonged tertiary stage, often obscuring the steady state creep regime, thereby complicating the interpretation of creep data [15].

In order to circumvent these problems, we have developed an apparatus for direct on-board testing of individual BGA solder balls via impression creep. The technique of impression creep wherein a flat-tipped cylindrical indenter is used to load the sample in nominal compression, allows steady state creep to be established within a relatively short time, with no subsequent appearance of a tertiary stage [16-20]. The approach requires minimal sample preparation, allows multiple creep curves to be generated from different solder balls within the same substrate, and can reliably replicate uniaxial creep data produced on bulk samples [16,17,21]. Furthermore, because of its ability to probe small material volumes, the technique is scaleable for testing of small microelectronic joints including both BGA and FC solder joints. The technique has been utilized to characterize the creep behavior of Sn-3.5Ag solder, using a recently developed apparatus based on a servo-hydraulic mechanical test frame in conjunction with a 1mm diameter tungsten carbide indenter [22]. In this article, we report on the miniaturization of the impression creep apparatus and approach for directly testing individual BGA solder balls (of 750μm diameter) attached to a commercial organic microelectronic packaging substrate, which is typically populated with numerous (~100-1000) solder balls. An example of a BGA substrate with solder balls is shown in Figure 1. The present work constitutes the first known report on the successful implementation of impression creep for testing non-bulk specimens.

II. INSTRUMENT DESIGN

1. System Overview

The miniaturized impression creep tester was developed by modifying an existing apparatus for impression creep testing of bulk specimens, which is described in detail elsewhere [22]. A detailed schematic of the miniaturized apparatus, which is described below, is shown in Figure 2.

A micro-machined, flat-tipped cylindrical tungsten carbide (WC) indenter of 100μm diameter (National Jet Co. Inc., LaVale, MD), mounted on a pin-chuck, was attached to a specially designed loading fixture made of INVAR, which was affixed to a servo-hydraulic test frame (Model 810, MTS System Corporation, Eden Prairie, MN). In order to maximize the displacement sensitivity of the test-frame, the hydraulic pressure was reduced four-fold from its default value to 6.89Pa. In order to obtain the desired load sensitivity, the test frame was equipped with a 2.5N tension/compression load transducer (Model 31, Honeywell Sensotec, Columbus, OH), allowing test stresses ranging from 2 to ~200 MPa to be applied on the specimen via the indenter. The servo-hydraulic dither of the test-frame (a continuous, small amplitude, high-frequency electrical pulse, ~550Hz, which is superimposed on the control waveform) was very carefully adjusted using a large indenter size (1mm diameter) and a stiff control sample (aluminum nitride, AlN) so that a load stability of around ±0.002N was obtained at all load levels of interest during constant load tests. This corresponds to a stress stability of ±0.25MPa for impression creep tests using a 100μm diameter punch.

A separate fixture made of INVAR, to which a linear-drive micrometer was attached, was used to measure the specimen displacement during a test, using a high temperature capacitance gauge affixed to the tip of the micrometer (see Figure 2). The capacitance gauge was calibrated for a full-scale displacement of 200μm with ±0.02μm stability at constant temperature (Model HPT40A, Capacitec, Ayer, MA), and used as target a polished stainless steel reference block, which was attached to the specimen stage. This fixture allowed separation of the displacement train from the load train, so that: (1) the weight of the micrometer-mounted capacitance gauge was not applied to the load cell, the capacity of which was kept deliberately small in order to enhance its load sensitivity; and (2) inadvertent loading of the load cell beyond its capacity

during adjustment of the micrometer to bring the capacitance gauge into reading range (~250μm) from the target at the start of every test could be avoided.

The specimen stage, on which the test sample is mounted, comprised an adjustable mounting platform for the specimen, which is attached to a dual-micrometer-controlled X-Y translation stage, which in turn is affixed to the servo-hydraulic ram of the test-frame. This arrangement allows a specific BGA ball in the specimen to be aligned accurately with the indenter in preparation for testing. A pair of 100mm x 50mm radiant heaters (100W each), located equidistantly on each side of the specimen and the reference block, was used to heat the sample to the test temperature, using a close-loop proportional controller (Model CNi8A33, Omega Engineering, Inc., Stamford, CT). The positioning of the heaters allowed the maintenance of identical temperatures at the specimen, the indenter, the reference block, and the capacitance gauge. An insulated ceramic enclosure mounted around the specimen stage on the non-moving platform below the X-Y translation stage constituted a specimen chamber. Two separate type-K thermocouples were utilized to measure the temperatures at the specimen / indenter and reference block / capacitance gauge within the specimen chamber. Additional thermocouples were utilized to measure the temperatures of the load cell, as well as the load and displacement fixtures during the test, which were all insulated from the ambient using ceramic fiber pads wrapped in a plastic sheet. The rationale for this, as well as other extreme precautions to maximize temperature stability, is discussed subsequently. Finally, the apparatus yielded load, displacement, and specimen temperature stabilities of ±0.002 N, ±0.02 μm and ±0.05K, respectively.

2. Temperature Control

During calibration of the apparatus, it became readily apparent that even when the specimen temperature was maintained constant to within ±0.05K, and a constant load was applied to a non-creeping control sample (AlN), significant time-dependent fluctuations were noted in the measured displacement reading. These fluctuations typically showed displacement variations ~0.2-0.4μm over periods of 20-60 minutes. These displacement variations were traced to be compound effects arising from ambient temperature changes, which caused thermal fluctuations at: (1) the load cell, causing the zero of the load cell to drift with time; (2) the load

and displacement train fixtures on which the load cell and capacitance gauges were mounted, causing the separate load and displacement trains to expand/contract slightly differently; (3) the entire mechanical test frame, to which all fixturing and the load-cell were attached, which in turn caused small fluctuations in the load/displacement fixtures via conduction; and (4) thermal fluctuations of the remotely-located amplifier box associated with the capacitance gauge, which caused fluctuations in the base reading of the capacitance gauge even without any real specimen displacement.

Since during an impression creep test, the displacement rate is directly proportional to the punch diameter [16], and for slowly creeping conditions, the total specimen displacement for a 100μm diameter indenter could be under 1μm during an entire test, it was deemed critical to eliminate the time-dependent fluctuations mentioned above. Accordingly, the following steps were taken. First, the load cell and the fixturing immediately above and below it were insulated from the ambient using fiberglass foam. While this enabled the load cell temperature to remain constant to within ±0.5K during a test following establishment of thermal equilibrium after heating the specimen to the test temperature, thereby eliminating the load cell zero-drift, it resulted in different steady-state load cell temperatures corresponding to different test temperatures. Since the calibration of the load cell depends on the operating temperature, this was compensated for calibrating it at different temperatures, and using different calibration constants at different test temperatures, for each of which the load-cell temperature was monitored with a separate thermocouple. Secondly, the separate load and displacement train fixtures were constructed from INVAR (an Fe-Ni alloy with a very low coefficient of thermal expansion, $\sim 0.5 \times 10^{-6}$/K), so that any differential expansion/contraction of the fixtures would have minimal impact on the measured displacement. Thirdly, the load and displacement train fixtures were thoroughly insulated from the ambient as noted earlier. Fourthly, large insulating walls of ceramic foam, covered with aluminum foil were placed around the entire setup comprising the load/displacement trains and the specimen stage/mounting platform and the exposed part of the servo-hydraulic actuator, as shown in the photograph of the apparatus in Figure 3. These outer walls help minimize heat losses due to any convection within the laboratory room, and the aluminum foil is used to minimize effects of external radiative heating [23]. Fifthly, all the unpainted metallic parts of the mechanical test-frame were wrapped with

plastic bubble-foam sheets, with an outer wrap of paper adhesive tapes, in order to minimize fluctuation of the load-frame temperature. Finally, the 2mm thick aluminum casing of the capacitance gauge amplifier was placed in contact with massive steel heat sinks on five sides (except the back, to which several wires were connected) in order to increase the thermal inertia of the amplifier to changes in ambient temperature. In addition, the ambient temperature of the test laboratory was kept as constant as possible with the available ventilation system, and by darkening all the windows of the room to minimize the impact of sunlight. With these changes, the systematic periodic oscillations in displacement were largely eliminated, producing a stable displacement reading to within ±0.02μm.

3. Video Imaging System

In order to facilitate precise placement of the sample feature of interest (in this case, the appropriate BGA solder ball) under the punch, a video imaging system was incorporated into the experimental apparatus. Since multiple solder balls need to be tested at a given temperature, this alignment needs to be achieved at the test temperature, which may range up to 453K for solders. In order to accomplish this, a high temperature gradient index lens (GRIN) in the form of a 0.6m long, 3mm diameter borescope encased in a thin stainless steel sheath (Hawkeye) was mounted on a commercial digital camcorder using an appropriate lens adapter. The camcorder in turn was connected to a video monitor, where the image could be observed and/or recorded as required. The front-end of the GRIN lens was placed within 5mm of the punch tip such that the punch tip and a few solder balls could be simultaneously imaged. This arrangement gave a magnification of ~8 times at the back-end of the lens, which was further magnified by the camcorder optics/electronics for imaging. The borescope-lens was inserted into the specimen chamber through small slots cut into the ceramic enclosure around the specimen, as well as the large aluminum wrapped insulation walls around the entire set-up (see Figure 3). A fiber-optic light source mounted inside a 6mm diameter metallic gooseneck with high-temperature epoxy was also inserted into the specimen chamber to provide illumination for imaging. A typical image from the video setup is shown in Figure 4.

In addition to enabling alignment of the indenter with the solder ball to be tested, the imaging system facilitates bringing the sample close to the indenter prior to testing. From the

two-dimensional video images, it is often difficult to visualize how close the indenter is to a given solder ball, both vertically as well as horizontally. Therefore, the illumination is placed in such a way relative to the indenter that the GRIN lens picks up the shadow of the indenter cast on the solder ball as they approach each other (Figure 4). The sample is brought towards the punch rapidly at the beginning till a shadow becomes visible (typically when the punch is ~100μm from the ball). Thereafter, the approach rate is lowered to ~2μm/s, and the position of the shadow relative to the punch tip is continuously monitored, enabling the operator to quickly align the test ball with the punch by translating the sample in the horizontal (i.e., X-Y) plane.

III. TESTING METHODOLOGY

A typical BGA substrate used in microelectronic packaging comprises a 25-50mm square organic substrate with multiple layers of internal electrical circuitry, populated on one surface with numerous (~100-500) solder balls, which are around 750 μm in diameter, as shown in Figure 1. One such BGA substrate with 90Pb-10Sn solder balls was sliced into several small (approximately 8mm x 17mm) dies. One such die was mounted on the specimen stage, which allows clamping of two opposite edges of the die. Prior to slicing the substrate into smaller dies, the top surfaces of the balls were slightly flattened in order to obtain a small level surface for impression creep testing.

Figure 5 shows a secondary electron (SE) image of the tip of the 100μm diameter WC punch which was used for impression creep testing. It is apparent that the punch is exactly right circular, with sharp edges, only slight surface scoring (<0.5μm deep). Although these surface marks may potentially affect the material response when the punch first contacts the specimen surface (due to localized plasticity in small regions before a fully developed plastic zone is formed under the entire punch-tip), their effect is minimized by the test methodology as described below.

Even though the tops of the balls were flattened prior to the test, the exact flatness is unknown. Furthermore, despite the best experimental care, it is very difficult to ascertain that the punch axis is exactly perpendicular to the specimen surface. This was evidenced in previous tests with a 1mm diameter punch [22], where the punch impressions on the specimen were often found to be gibbous even after prolonged testing at low loads/temperatures, although the

specimen was mounted on a self-leveling specimen stage. This results in an exaggerated primary stage, making the establishment of a true steady state creep response difficult in reasonable time. In order to circumvent this problem, the following test methodology was adopted in the present BGA tests. Following initial contact between the punch and the specimen, the load is increased slowly, making the punch penetrate into the sample by a nominal depth of ~7-10μm (corresponding to an applied punch stress σ_p of ~50-60MPa) in order to ensure complete contact between the punch tip and the sample. This procedure not only allows the establishment of complete contact between the punch and sample, but also creates a fully developed plastic zone under the punch. Prior analytical work [24] has shown that the existence of fully developed plastic zone under the punch is critical to the rapid establishment of a steady state Von-Mises effective stress distribution under the punch, and hence a steady-state impression velocity, during subsequent creep testing, thereby substantially shortening the required experimental time [24]. This procedure obviously generates a heavily dislocated structure that is not consistent with the dislocation structure at steady-state creep for lower applied stresses, and the original structure must be recovered. Therefore, immediately after initial penetration to develop the plastic zone under the punch, the applied punch stress is reduced to 1 MPa, and held constant at the test temperature for 3-5 hours in order to allow the plastic zone to recover partially. This recovery time is allowed in order to prevent the appearance of a negative creep rate, which is sometimes observed at the initial stages of a stress-decrease creep test while the microstructure adjusts to the new, lower stress level [25]. Subsequently, the applied stress is increased to the test stress and held constant to produce the requisite creep curve.

Example load vs. time and displacement vs. time plots during (a) the initial approach and contact, (b) initial penetration and unloading, (c) the recovery stage following load reduction, (d) loading to the creep stress, and (e) the actual creep test at 323K and σ_p=32MPa, are shown in Figure 6 in order to elucidate the testing methodology. Here, the punch stress σ_p (given by applied force per unit punch cross sectional area) is about 3-3.5 times the equivalent uniaxial compressive stress, depending on the specific material properties [24,26]. The indentation (i.e., punch impression) on the flattened top surface of the solder ball following a test is shown in Figure 7, indicating that (i) the impression can be located quite precisely on the roughly 300μm diameter flattened region at the top of the ball using the present apparatus, and (ii) the initial

penetration assures complete contact between the punch and sample, even though the top of the ball may be slightly inclined with respect to the punch-axis.

IV. RESULTS AND DISCUSSION

1. Substrate Creep Effect

In any mechanical testing experiment, it is important to ascertain that the measured displacements represent the specimen deformation, rather than being artifacts associated with the testing apparatus. Although effects due to machine compliance were determined to be negligible by testing a control AlN sample at high loads with a large (i.e., 1mm diameter) indenter, it was deemed that part of the measured displacement may be due to elastic and/or viscoelastic deformation of the organic BGA substrate. Indeed, organic substrates with attached solder balls are known to be slightly warped due to residual stresses induced during solder reflow. Since this curvature is temperature dependent (as clear from the shadow Moiré measurements at 293K and 398K, shown in Figure 8), and can relax or increase over time under the applied punch stress during an elevated temperature creep test, it can potentially obfuscate the measured creep displacements. This is particularly so when the substrate curvature relaxation/increase rate is comparable to the creep rate of the solder. Consequently, experiments were performed in order to compare the displacement rates obtained by impressing the substrate, with that of the solder.

In order to compare the time-dependent deformation of the substrate with the creep of the solder, two tests were conducted on the substrate right next to several tested solder balls under the following conditions: (a) at T=323K, σ_p=10.1MPa; (b) at T=423K, σ_p= 26.4MPa. These two tests roughly bracket the least and the most aggressive conditions, respectively, under which the solder balls were tested. In actuality, when the solder ball is creep tested under a punch stress of σ_p, the equivalent punch stress experienced by the substrate is only $\sigma_p/25$, since the applied force is transmitted to the substrate through the bottom of the solder ball, which is ~5 times greater in diameter than the 100μm diameter punch (see Figure 1). Therefore, the substrate creep rates obtained from these tests represent highly aggressive estimates. The same punch forces were employed for the substrate tests since the resolution of the load cell made it difficult to apply the very small forces necessary to produce the actual stresses experienced by the substrate.

Figures 9a and 9b illustrate displacement vs. time plots obtained from the substrate and the solder/substrate combination, for the two different test conditions (a and b). Since the substrate is warped, the substrate creep curves were found to be position dependent, being the slowest close to the clamped edges. The curves shown in Figure 9 represent the fastest creep curves recorded for the substrate. It is clear that the net displacement and displacement rate of the solder/substrate combination are significantly greater than those of the substrate for both conditions. This is despite the fact that the punch stresses in the substrate tests are about 25 times greater than the actual stresses to which the substrate is subjected during solder tests. This is because during a solder creep test, the applied load is transmitted to the substrate through the bottom of the solder ball, which contacts the substrate over a circle of 5 times greater diameter than the punch. Therefore, the actual contribution of the substrate to solder/substrate deformation is expected to be much smaller than it appears in Figure 9. These results indicate that for the present material, the effect of substrate creep on the measured solder creep behavior is negligible. This suggests that even if the substrate is significantly warped, the impact of substrate creep can be largely eliminated by cutting the substrate into small pieces (in order to reduce the in-plane residual stresses, and therefore the curvature), and clamping the edges of the test piece tightly to the specimen stage (in order to keep the substrate as flat as possible).

2. Creep Data for Solder

Figure 10 shows several sample creep curves of the 90Pb-10Sn BGA solder balls under different testing conditions. Clearly, steady state creep is established quite quickly (within 1-3 hours, depending on testing condition), and the curves show extended secondary creep without a tertiary stage. Thus entire creep curves may be generated within 5-6 hours, unlike conventional creep tests, which take much longer. This, as discussed earlier, is not only advantageous for minimizing *in situ* microstructural changes (e.g., coarsening) during testing, but also for enhancing the throughput of test results so that several separate creep tests can be accomplished on one sample (i.e., one small piece of substrate with several balls) within the time that would be necessary for one or two conventional tests.

For power law creep behavior, the steady state impression velocity is given by:

$$V = A' f(\phi)\left(\frac{Gb}{kT}\right)\left(\frac{\sigma_p}{G}\right)^n e^{-\frac{Q}{RT}} \qquad (1)$$

where $\sigma_p \approx 3.5 \times$ the equivalent uniaxial stress (σ), the constant A' incorporates the Dorn constant A, as well as a factor to convert σ to σ_p, and $f(\phi)$ is a function of the punch diameter ϕ such that $\dot{\delta}/f(\phi)$ is the average creep strain rate in the plastic zone under the punch. It has been shown that the parameter $f(\phi)$, representing the depth of the plastic zone under the indenter, stays approximately constant and equal to ϕ during steady state creep [26]. Thus, since A', $f(\phi)$, b and k are constants,

$$\frac{VT}{G} \propto \left(\frac{\sigma_p}{G}\right)^n e^{-\frac{Q}{RT}} \qquad (2)$$

This allows us to obtain the activation energy Q from a plot of ln[VT/G] vs. 1/T at constant σ_p/G, and the stress exponent n from a plot of ln[VT/G] vs. σ_p/G at constant T.

Figure 11a shows a plot of the quantity V(T/G) versus modulus compensated punching stress (σ_p/G) at two temperatures (323K and 348K). At both temperatures, a power-law behavior with $n \approx 4$ is noted. Figure 11b shows plots of ln[V (T/G)] vs. 1/T at a constant σ_p/G value of 0.01. The activation energy Q is 43kJ/mole. In previous tensile creep studies on bulk Pb-10Sn alloys over 273K to 373K [28], n was observed to increase gradually from 3 at the lower temperatures to ~5 at the higher temperatures, although no rationale for this variation was offered. However, this is in general agreement with n~4 obtained in the present study over the temperature range of 323-373K. Diffusivity measurements of Pb in itself and in Pb-Sn alloys using the Whipple-Suzoka analysis [29,30] have shown that in the sub-solvus region for the present material (i.e., <398K), the expected Q value should be ~80kJ/mole for volume diffusion (Q_{vol}), and between 30 and 40 kJ/mole for grain boundary diffusion, the lower value being expected for Sn concentrations above 5wt.%. Although corresponding Q values for dislocation core diffusion (Q_{core}) are not available, it is expected to be between $0.6Q_{vol}$ and Q_{gb}, i.e., between 48kJ/mole and 30kJ/mole. Therefore, our activation energy value of 43kJ/mole is in good agreement with the expected Q_{core} in Pb. Thus, the impression creep results presented here suggest that 90Pb-10Sn BGA balls creep by dislocation core diffusion controlled power-law

creep, with the rate limiting mechanism being dislocation climb. This is consistent with available creep data on bulk high-lead solders at sub-solvus temperatures [28].

V. Conclusions

An apparatus for miniaturized impression creep testing of tiny solder balls, attached to a microelectronic packaging substrate, was developed. This approach allows testing of individual solder balls on a substrate, and can therefore discern differences between the properties of different balls (e.g., due to defects), unlike other tests designed for microelectronic solder (e.g., lap-shear), which yield properties averaged over a large array of balls. The test is relatively rapid, with steady state creep being established well within 3-5 hours, and shows no tertiary stage. Furthermore, no special sample preparation is required for the test. The test is thus well suited for situations where a high throughput of creep data at low net cost is desirable, e.g., in currently ongoing evaluations of a wide range of lead-free solder candidate materials. The apparatus reported here was successfully designed and implemented to test nominally 750μm diameter BGA solder balls, using a 100μm diameter cylindrical WC punch. The test is further scaleable for testing of smaller flip-chip (FC) joints, using a smaller punch. The temperature, load and displacement stabilities of the instrument have been carefully optimized to meet the testing requirements. A video imaging system facilitates precise alignment and placement of the indenter on the specimen at the test temperature. The possible effect of substrate curvature on the experimental solder creep curves was evaluated and was deemed to be insignificant when the substrate is cut into small pieces to minimize its internal residual stresses. It was found that for the high displacement resolutions (±0.02μm) required, the most critical experimental parameter to control was the thermal stability of the entire load and displacement trains, as well as the capacitance gauge amplifier. Initial impression creep data on 90Pb-10Sn BGA solder balls are reported, and these data were found to be consistent with test results on the same alloy based on bulk samples. The present work constitutes the first known report on the successful implementation of impression creep for testing non-bulk specimens.

ACKNOWLEDGEMENTS

This work is supported by an NSF-GOALI program in partnership with INTEL Corporation (grant # DMR-0209464) and SRC contract # 2002-NJ-1004. The collaboration and support of Drs. R. Mahajan and Fay Hua of INTEL are gratefully acknowledged. The authors would like to thank Mr. M. Mello for his help in measuring substrate curvatures, Dr. A. Gopinath for useful discussions, and Mr. Tom Christian for his technical assistance in apparatus design. Discussions with Dr. Vijay Sarihan of Motorola during the early stages of conceptual development of the test are also gratefully acknowledged.

References

1. H.G. Song, J.W. Morris Jr., F. Hua, "Anomalous Creep of Sn-Rich Solder Joints", *Materials Transactions*, **43**, 1847, 2002.

2. W. Yang, L.E. Felton, R.W. Messler, "The Effect of Soldering Process Variables on the Microstructure and Mechanical Properties of Eutectic Sn-Ag/Cu Solder Joints", *J. Electronic Mater.*, **24**, 1465, 1995.

3. M.D. Mathew, S. Movva, H. Yang, K.L. Murty, "Creep of Sn, Sn-3.5Ag and Sn-5Sb Solders for Electronic Packaging", in *Creep Behavior of Advanced Materials for the 21st Century*, ed. R.S. Mishra, A.K. Mukherjee, and K.L. Murty, TMS, 51, 1999.

4. M.L. Huang, L. Wang, C.M.L. Wu, "Creep Behavior of Eutectic Sn-Ag Lead-free Solder Alloy", *J. Mater. Res.*, **17**, 2897, 2002.

5. K. Wu, N. Wade, J. Cui, K. Miyahara, "Microstructural Effect on the Creep Strength of a Sn-3.5%Ag Solder Alloy", *J. Electronic Mater.*, **32**, 5, 2003.

6. Onofrio A. Anastasio, "An Approach For Impression Creep Of Pb-free Microelectronic Solders", M.S. Thesis, Department of Mechanical Engineering, Naval Postgraduate School, Monterey, CA, 2002.

7. P.T. Vianco, J.A. Rejent, and A.C. Kilgo, "Time-Independent Mechanical and Physical Properties of the Ternary 95.5Sn-3.9Ag-0.6Cu Solder", *J. Electronic Mater.* **32,** 142, 2003.

8. I. Dutta, "A Constitutive Model for Creep of Lead-Free Solders Undergoing Strain-Enhanced Microstructural Coarsening: A First Report", *J. Electronic Mater.*, 32, 201, 2003.

9. W. Yang, R.W. Messler, L.E. Felton, "Microstructure Evolution of Eutectic Sn-Ag Solder Joints", *J. Electronic Mater.*, **23**, 765, 1994.

10. P. Hacke, A. F. Sprecher, H. Conrad, "Computer Simulation of Thermo-Mechanical Fatigue of Solder Joints Including Microstructure Coarsening", *J. Electronic Packaging*, **115**, 153, 1993.

11. H. Conrad, Z. Guo, Y. Fahmy, D. Yang, “Influence of Microstructure Size on the Plastic Deformation Kinetics, Fatigue Crack Growth Rate, and Low-Cycle Fatigue of Solder Joints”, *J. Electronic Mater.*, **28**, 1062, 1999.

12. H. Yang, P. Deane, P. Magill and K. Linga Murty, "Creep Deformation of 96.5Sn-3.5Ag Solder Joints in a Flip Chip Package", Proc. ECTC, 1996, pp. 1136-1142.

13. R. Darveaux, K. Banerji, “Constitutive Relations for Tin-Based Solder Joints”, IEEE Trans. Comp. Hyb. Manuf. Technol., 15, 1992, pp.1013-1024.

14. H.L. Reynolds, S.H. Kang, J.W. Morris, “The Creep Behavior of In-Ag Eutectic Solder Joints”, J. Electronic Mater., 28, 1999, pp. 69-75.

15. K.L. Murty, H.Yang, P. Deane, P. Magill, “Deformation Mechanism in Sn-Based Solder Materials”, Proc. Interpack ’97: Adv. in Electronic Comp. Tech. Conference, 1996, pp. 1136-1142.

16. S.N.G. Chu and J.C. M. Li, "Impression Creep: A new creep test", J. Mater. Sci., 12, 1977, pp. 2200-2208.

17. E.C. Yu and J.C. M. Li, "Impression creep of LiF single crystals", Phil. Mag., 34, 1977, p. 811.

18. F. Yang and J.C. M. Li, "Impression creep of a thin film by vacancy diffusion. I. Cylindrical Punch", J. Appl. Phys., 74, 1993, pp. 4390-4397.

19. D. Chiang and J.C. M. Li, "Impression creep of lead", J. Mater. Res., 9, 1994, pp. 903-908.

20. F. Yang and J.C.M. Li, "Impression test of 63Sn-37Pb eutectic alloy", Mater. Sci. Eng., A201, 1995, pp. 40-49.

21. D. Dorner, K. Roller, B. Skotzki, B. Stockhert and G. Eggeler, "Creep of a TiAl alloy: a comparison of indentation and tensile testing", Mater. Sci. Eng. A, 2003, in press.

22. I. Dutta, C. Park, S. Choi, “Impression Creep Characterization of Rapidly Cooled Sn-3.5Ag Solders”, *Mater. Sci. Eng. A*, in press.

23. A. Gopinath, private communication, Naval Postgraduate School, Monterey, CA, 2003.

24. D. Pan and I. Dutta, “A Complication of Impression Creep Tests and its Solution: Application to Sn-3.5Ag Solders”, *Materials Science and Engineering A*, in press.

25. R.W. Evans, B. Wilshire, “Creep of Metals and Alloys”, The Institute of Metals, 1985.

26. F. Yang, J.C.M. Li and C.W. Shih, "Computer simulation of impression creep using the hyperbolic sine stress law", Mater. Sci. Eng., A201, 1995, pp. 50-57.

27. H.J. Frost and M.F. Ashby, "Deformation Mechanism Maps - The Plasticity and Creep of Metals and Ceramics", Pergamon Press, Oxford, 1982, pp. 21.

28. H.J.Frost, R. T. Howard, P.R. Lavery, S. D. Lutender, “Creep and Tensile Behavior of Lead-Rich Lead-Tin Solder Alloys”, IEEE Trans. Comp. Hyb. Manuf. Technol., 11, 1988, pp. 371-379.

29. D. Gupta and K.K. Kim, "Grain boundary self diffusion in Pb", J. Appl. Phys., 51, 1980, pp. 2066-2069.

30. J. Oberschmidt, K.K. Kim and D. Gupta, "Grain boundary diffusion in some Pb-Sn alloys", J. Appl. Phys., 53, 1982, pp.5672-5677.

List of Figures:

Figure 1. Schematic of (a) BGA balls on an organic substrate and (b) a cross section of a single solder ball.

Figure 2: Schematic of the experimental apparatus for minaturized impression creep of BGA balls, showing the indenter, sample, the separate load and displacement trains, and the micrometer-controlled sample stage. The gray area behind the sample represents one of a pair of radiant heaters. For clarity, the GRIN lens of the viewing system, which extends into the hot specimen chamber with its tip within 4-5 mm of the indenter and sample, is not shown.

Figure 3: Photograph of experimental arrangement with the front insulating guard removed, showing the insulated load and displacement trains, the borescope GRIN lens and the fiber optic light source extending into the heated ceramic-enclosed sample chamber. The borescope lens is attached to a video recorder which is connected to a TV monitor (not shown).

Figure 4: A representative digital still image from the video setup used for aligning the indenter with the solder balls. The indenter, which is seen at the top, is observed to cast a shadow on the flattened top surface of the BGA ball under it. The relative positions of the indenter tip and shadow facilitates precise placement of the punch on the ball.

Figure 5: Secondary electron image of the tip of a 100μm diameter cylindrical WC punch.

Figure 6: Example load vs. time and displacement vs. time plots during (a) the initial approach and contact, (b) initial penetration and load reduction, (c) the recovery stage following load reduction, (d) loading to the creep stress, and (e)the actual creep test at 323K and σ_p=32MPa.

Figure 7: Secondary electron image of a BGA solder ball after impression creep testing, showing a punch impression on the flattened part (roughly 400 μm diameter) at the top surface of the ball. A pile-up of the solder material displaced from the sample by the punch is also seen around the perimeter of the impression.

Figure 8: Maps of out-of-plane deflections (in μm) of a BGA substrate at (a) 298K and (b) 423K, as obtained by shadow Moiré measurements. The maximum vertical deflection of the substrate is 26 μm at 298K, and 31μm at 423K. The curvature, and hence the out-of-plane displacements, are functions of temperature.

Figure 9: The substrate creep effect at: (a) σ_p=10.1MPa, T=50°C; (b) σ_p=26.4MPa, T=150°C. The curves illustrate the time-dependent response of the substrate and the solder ball on substrate under the same punch stresses. However, it should be noted that the stress applied to the substrate during a solder creep test is ~1/25 of the punch stress applied to the solder, since the bottom diameter of the solder ball is ~5 times the punch diameter.

Figure 10: Example creep curves of 90Pb-10Sn BGA solder balls under different testing conditions. Steady state creep is established within 1-3 hours for all testing conditions.

Figure 11: (a) Punch stress dependence of impression velocity, showing n~3.8-4.

(b) Temperature dependence of impression velocity, showing that Q≈43kJ/mole.

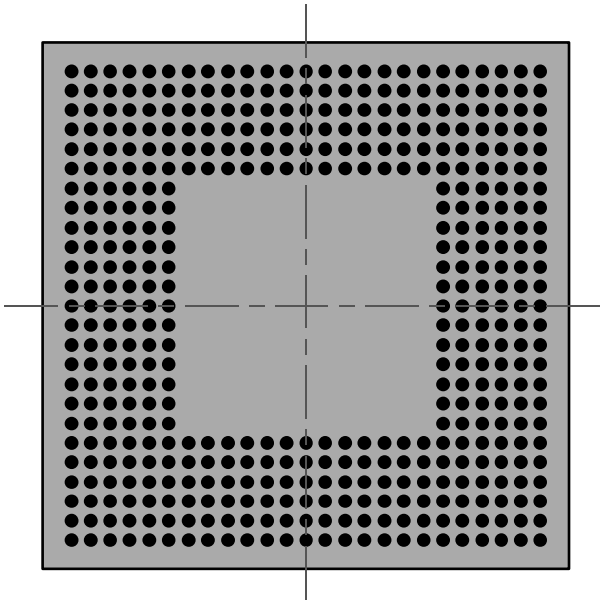

(a)

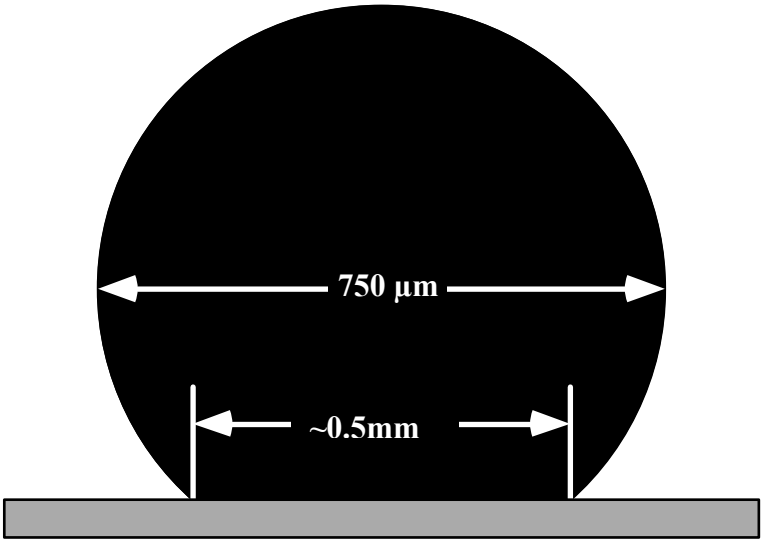

(b)

Figure 1. Schematic of (a) BGA balls on an organic substrate and (b) a cross section of a single solder ball.

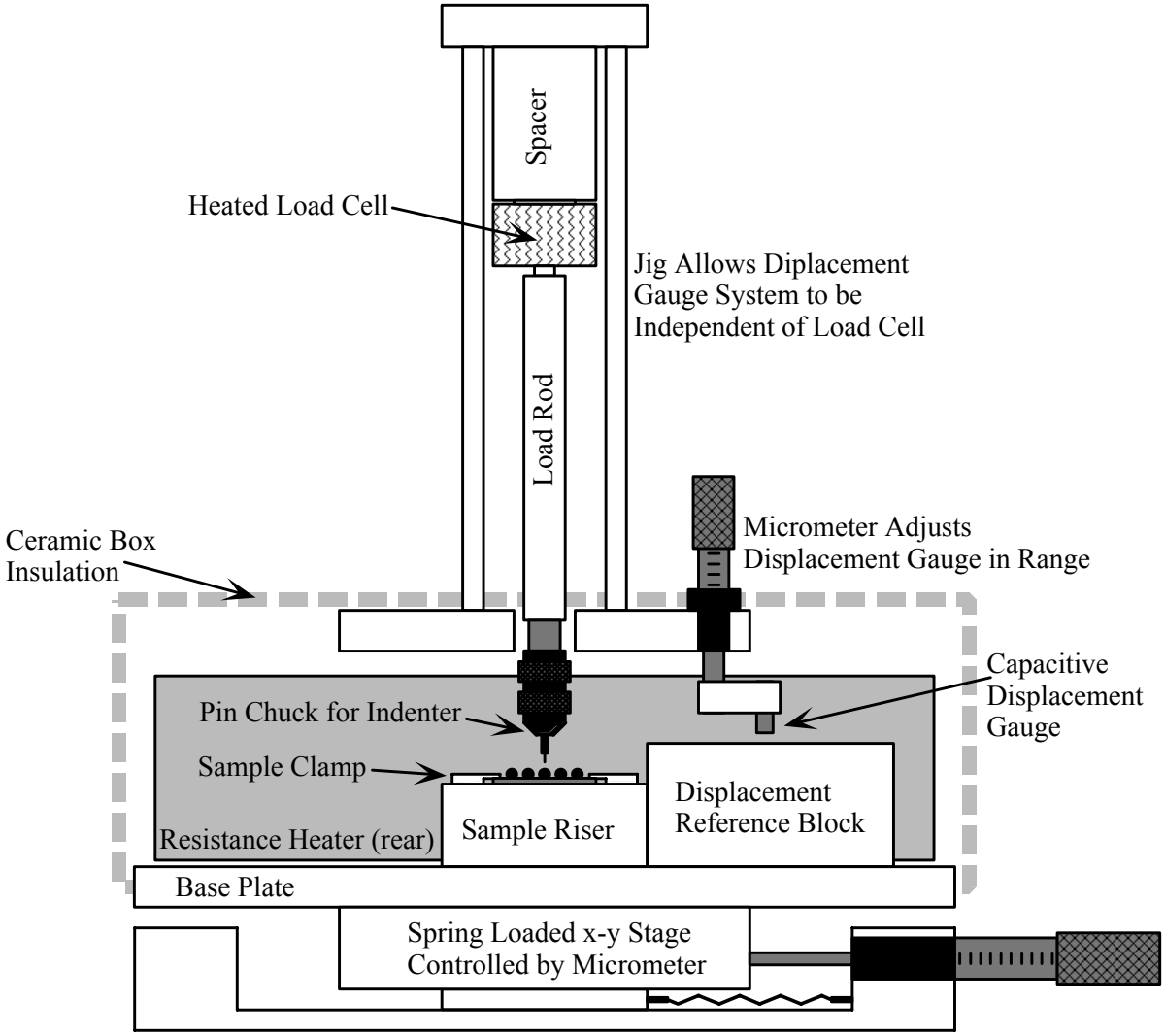

Figure 2: Schematic of the experimental apparatus for minaturized impression creep of BGA balls, showing the indenter, sample, the separate load and displacement trains, and the micrometer-controlled sample stage. The gray area behind the sample represents one of a pair of radiant heaters. For clarity, the GRIN lens of the viewing system, which extends into the hot specimen chamber with its tip within 4-5 mm of the indenter and sample, is not shown.

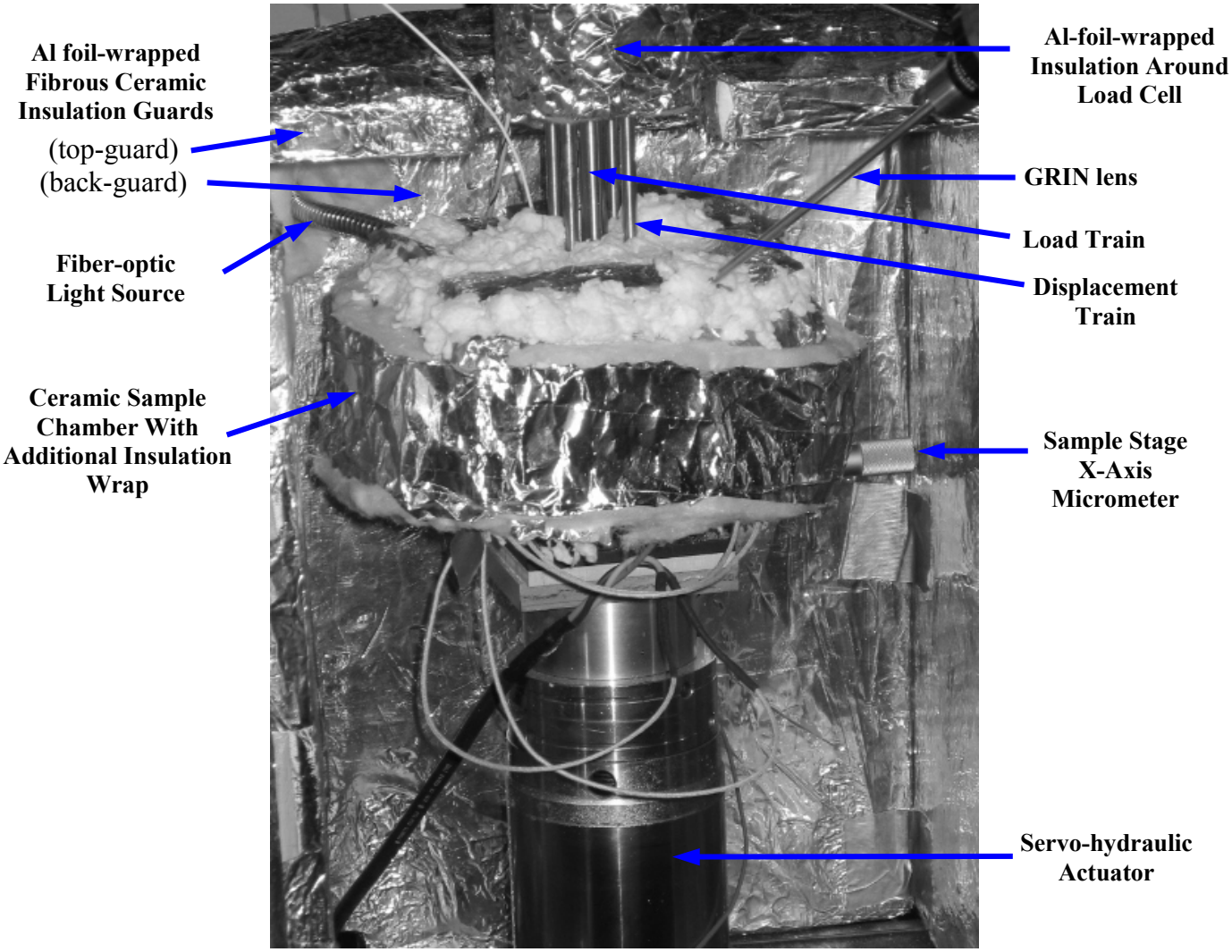

Figure 3: Photograph of experimental arrangement with the front insulating guard removed, showing the insulated load and displacement trains, the borescope GRIN lens and the fiber optic light source extending into the heated ceramic-enclosed sample chamber. The borescope lens is attached to a video recorder which is connected to a TV monitor (not shown).

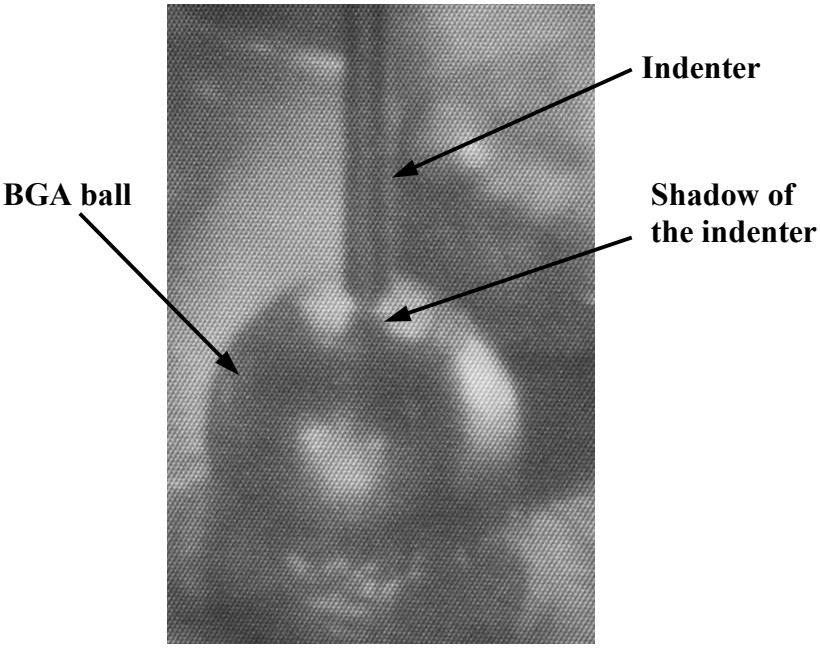

Figure 4: A representative digital still image from the video setup used for aligning the indenter with the solder balls. The indenter, which is seen at the top, is observed to cast a shadow on the flattened top surface of the BGA ball under it. The relative positions of the indenter tip and shadow facilitates precise placement of the punch on the ball.

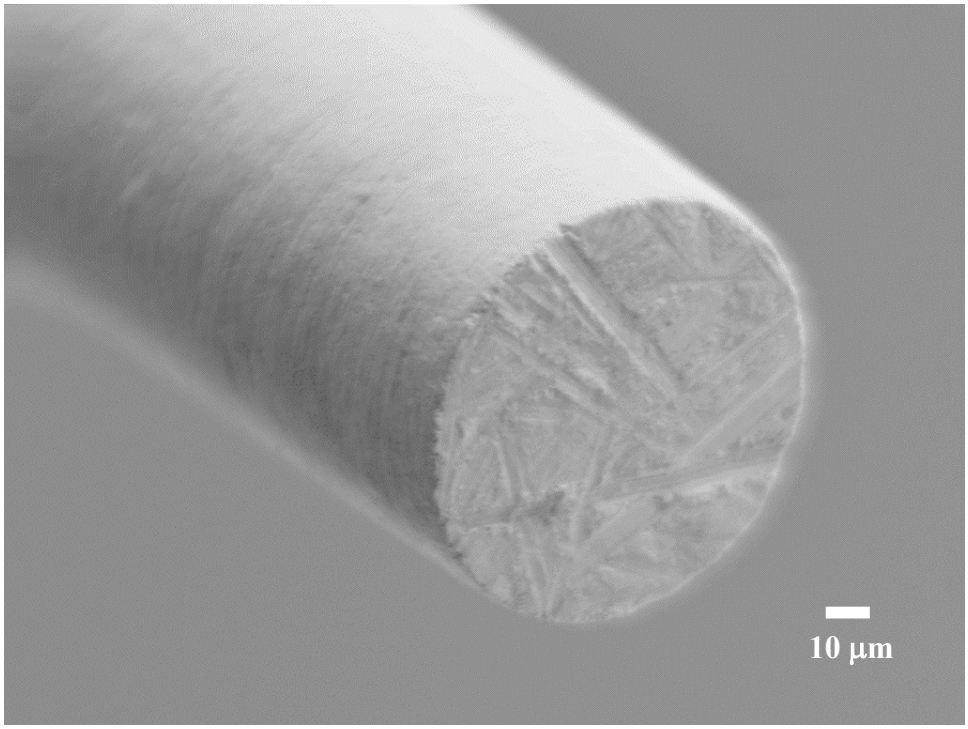

Figure 5: Secondary electron image of the tip of a 100μm diameter cylindrical WC punch.

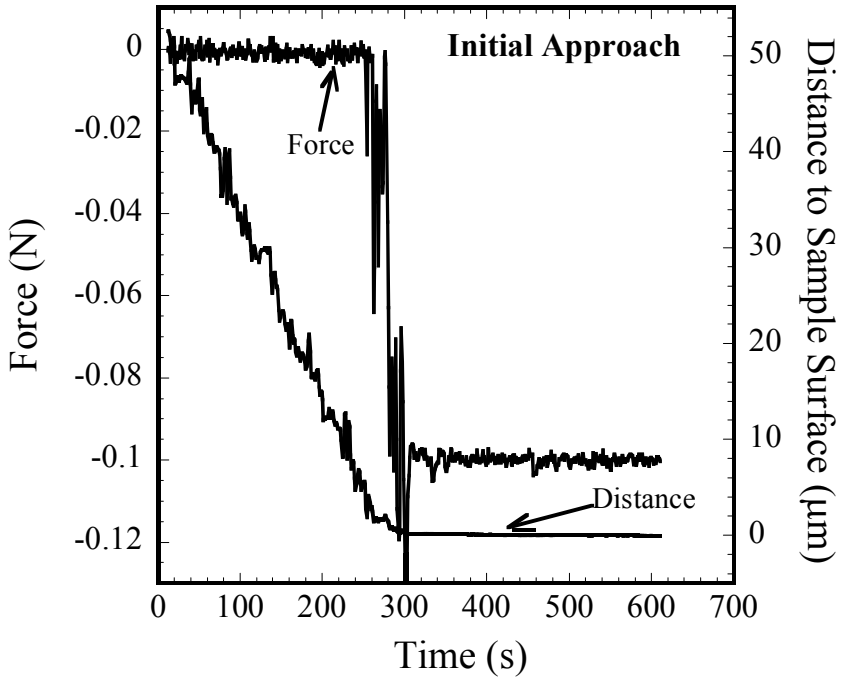

(a)

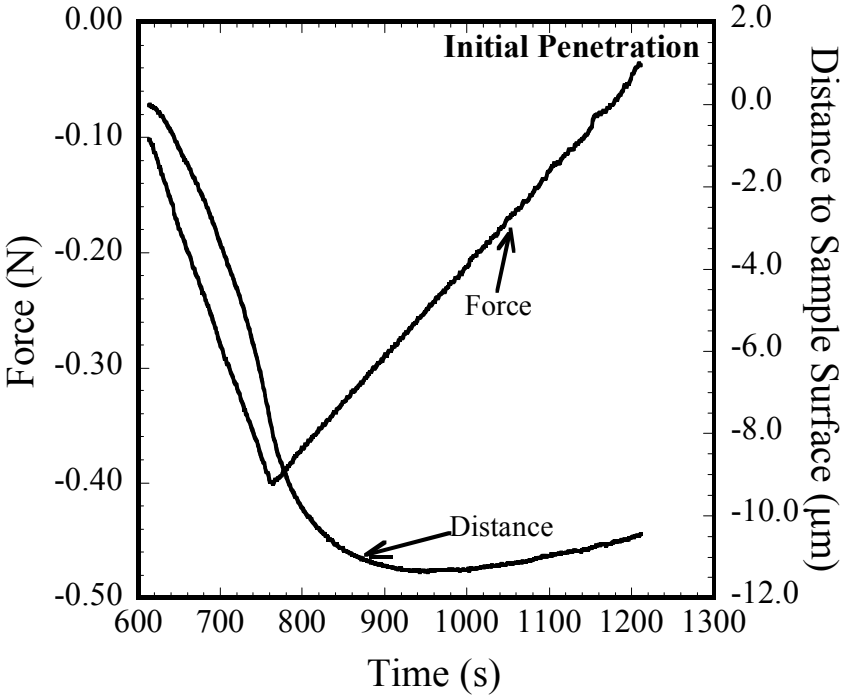

(b)

Figures 6 (a) and 6(b)

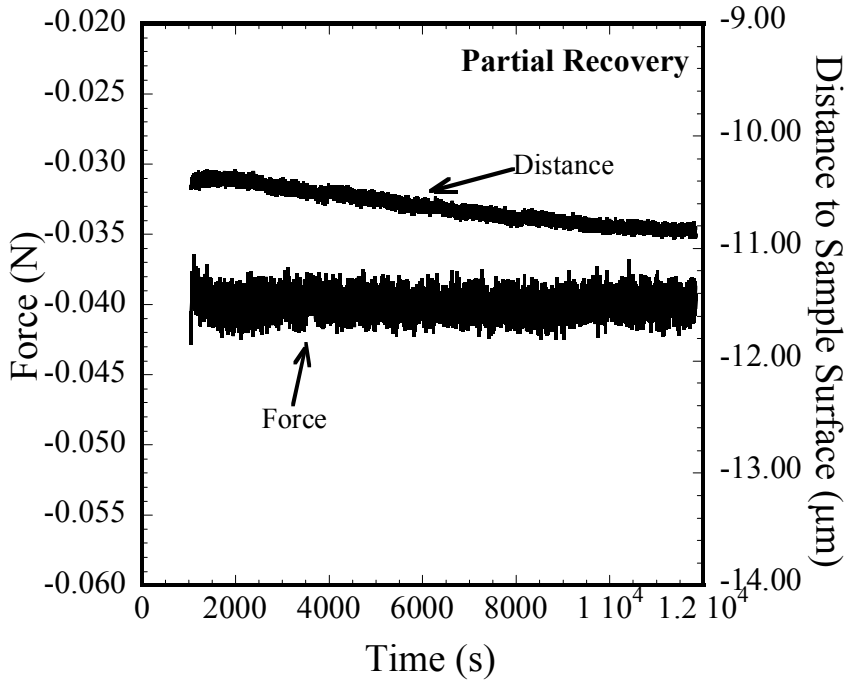

(c)

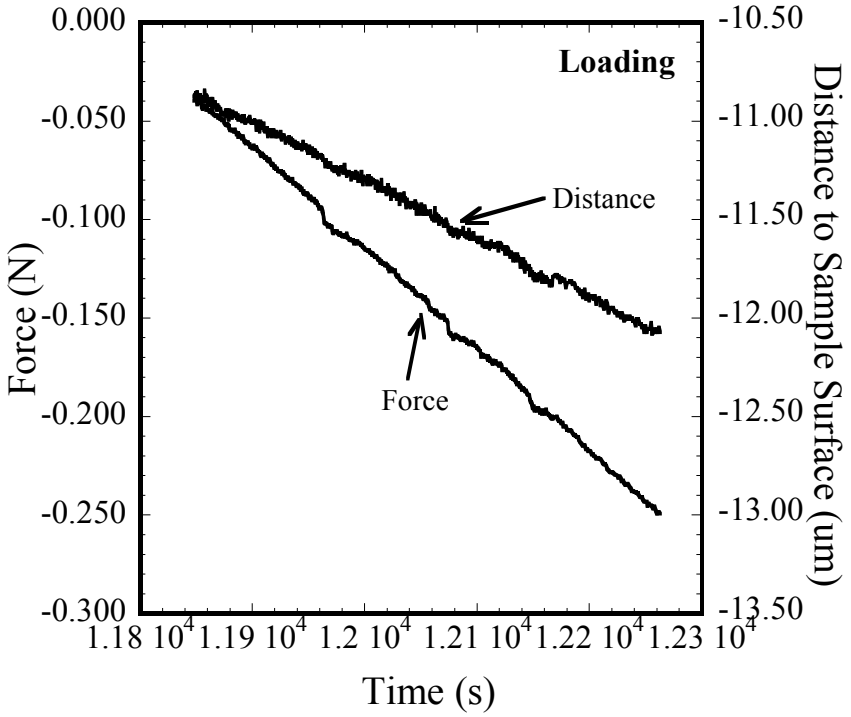

(d)

Figures 6(c) and 6(d)

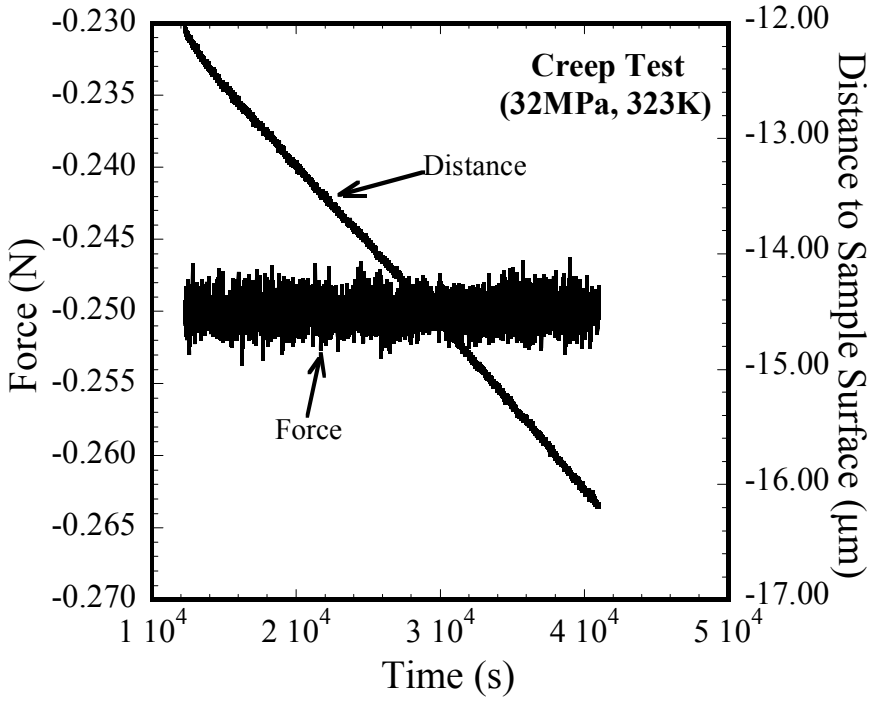

(e)

Figure 6: Example load vs. time and displacement vs. time plots during (a) the initial approach and contact, (b) initial penetration and load reduction, (c) the recovery stage following load reduction, (d) loading to the creep stress, and (e)the actual creep test at 323K and σ_p=32MPa.

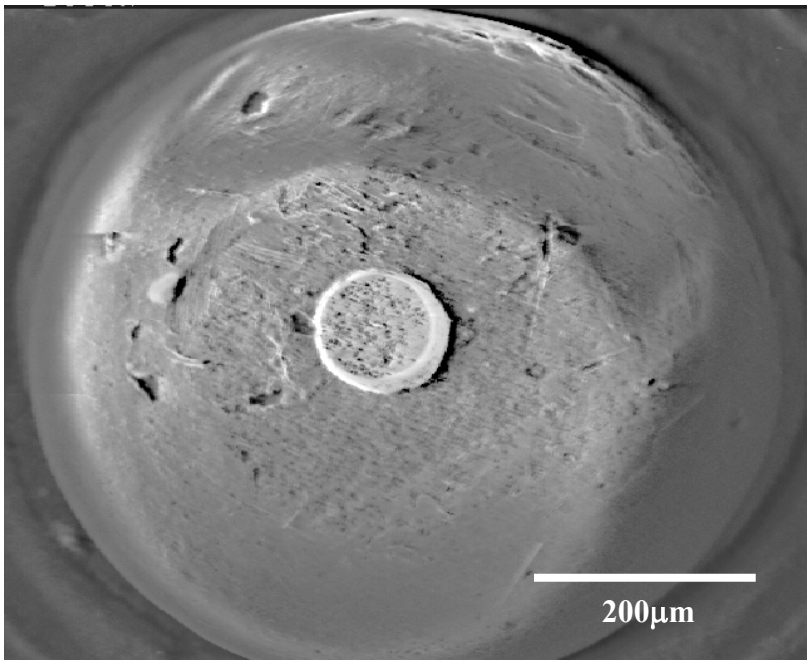

Figure 7. Secondary electron image of a BGA solder ball after impression creep testing, showing a punch impression on the flattened part (roughly 400 μm diameter) at the top surface of the ball. A pile-up of the solder material displaced from the sample by the punch is also seen around the perimeter of the impression.

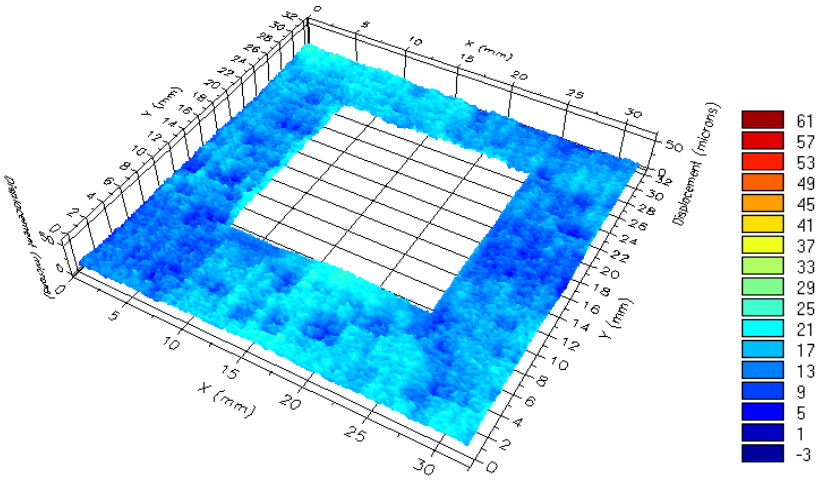

Maximum Deflection = 26 microns

(a)

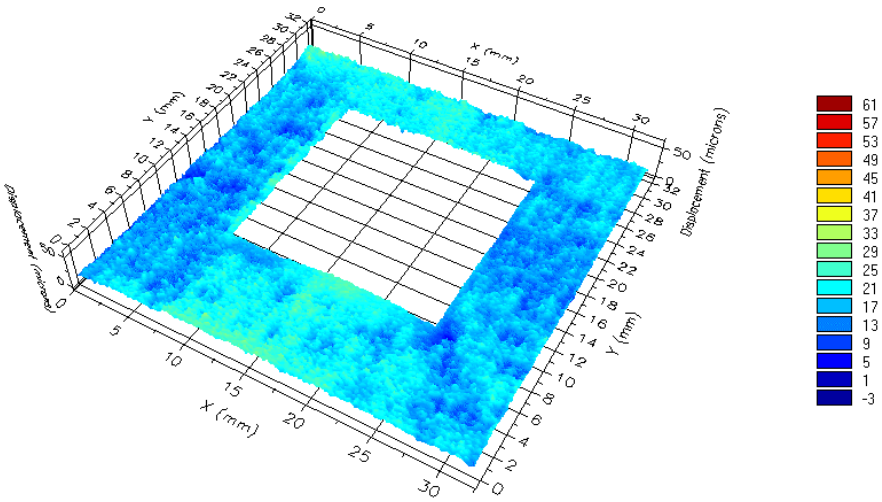

Maximum Deflection = 31 microns

(b)

Figure 8: Maps of out-of-plane deflections (in μm) of a BGA substrate at (a) 298K and (b) 423K, as obtained by shadow Moiré measurements. The maximum vertical deflection of the substrate is 26 μm at 298K, and 31μm at 423K. The curvature, and hence the out-of-plane displacements, are functions of temperature.

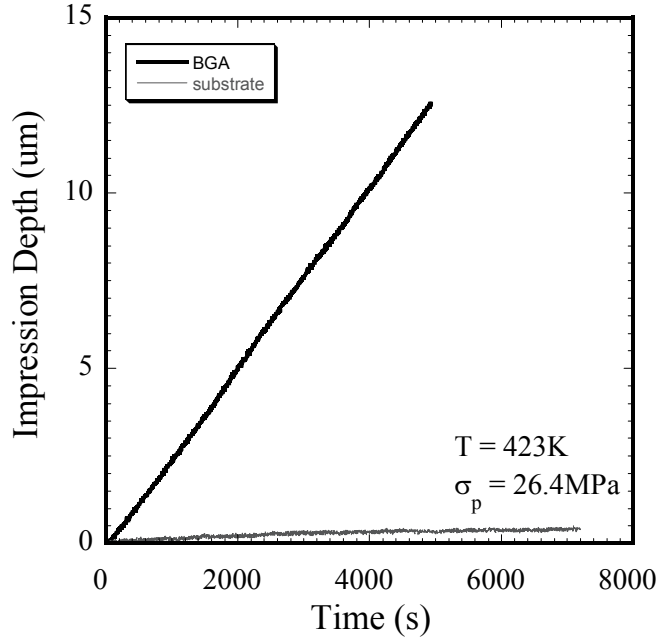

(a)

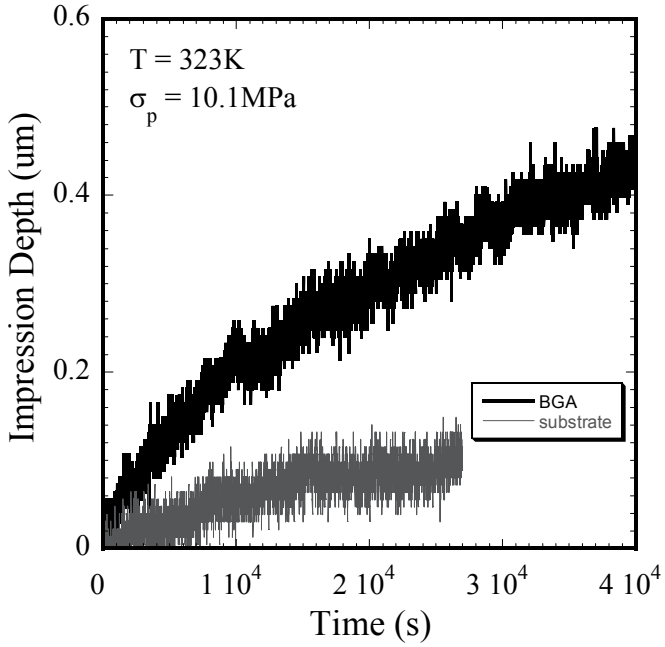

(b)

Figure 9: The substrate creep effect at: (a) σ_p=10.1MPa, T=50°C; (b) σ_p=26.4MPa, T=150°C. The curves illustrate the time-dependent response of the substrate and the solder ball on substrate under the same punch stresses. However, it should be noted that the stress applied to the substrate during a solder creep test is ~1/25 of the punch stress applied to the solder, since the bottom diameter of the solder ball is ~5 times the punch diameter.

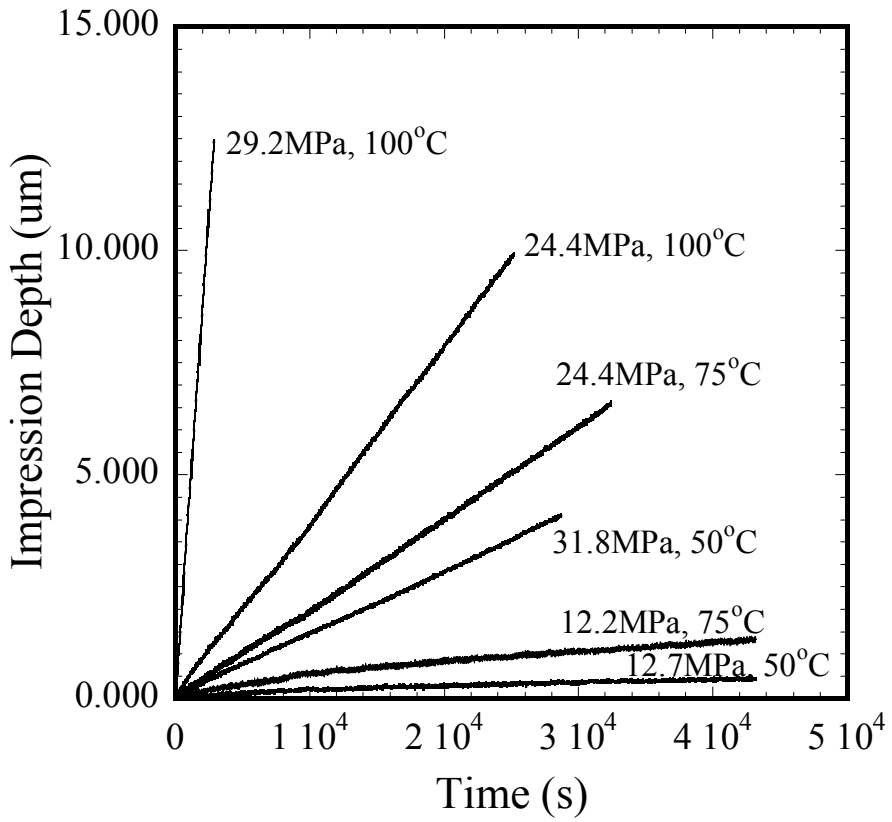

Figure 10: Example creep curves of 90Pb-10Sn BGA solder balls under different testing conditions. Steady state creep is established within 1-3 hours for all testing conditions.

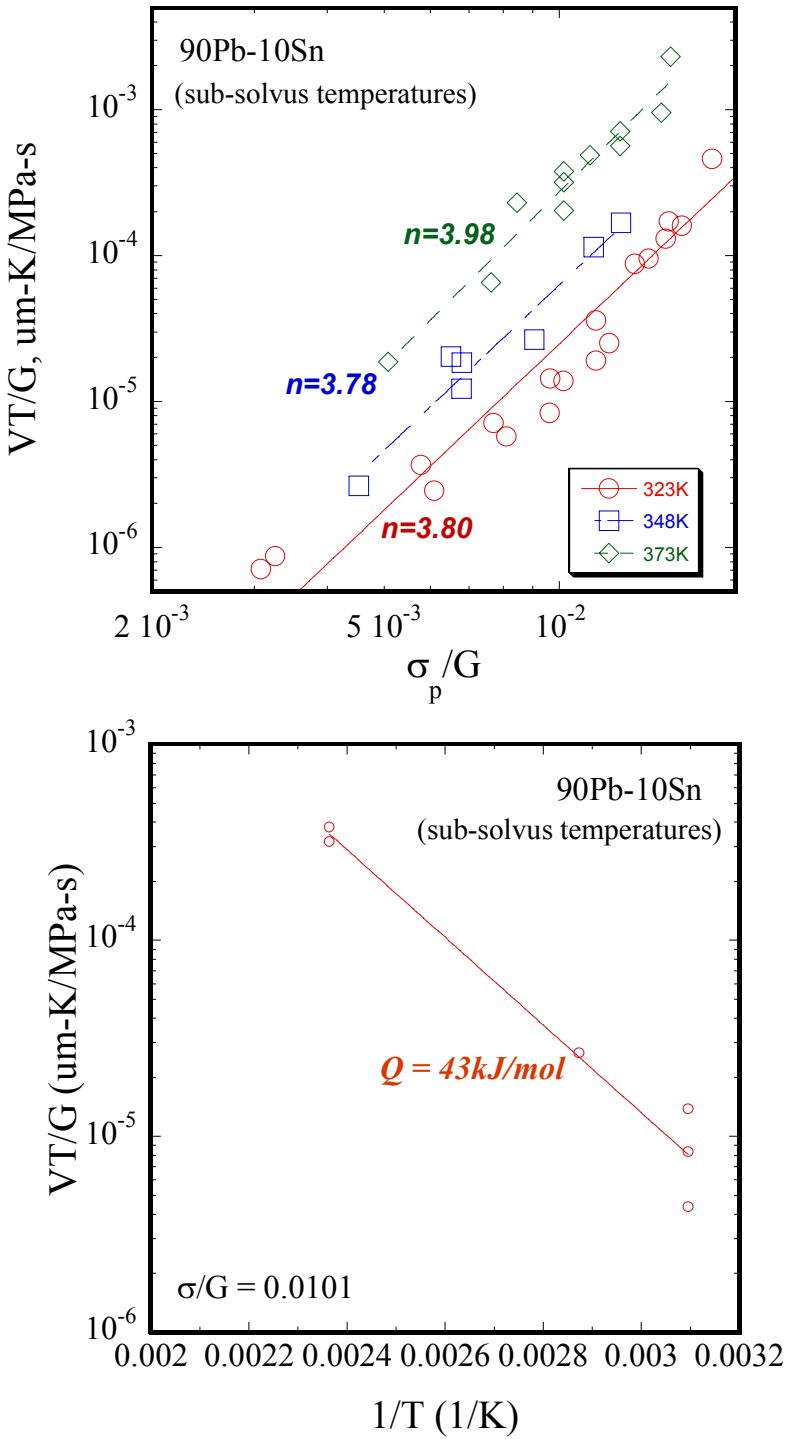

Figure 11: (a) Punch stress dependence of impression velocity, showing n~3.8-4.

(b) Temperature dependence of impression velocity, showing that Q≈43kJ/mole.